Explaining Inaccurate Predictions of Models through k-Nearest Neighbors

Zeki Bilgin[1][a] and Murat Gunestas[2][b]
[1]*Arcelik Research, Istanbul, Turkey*
[2]*Cyphore Cyber Security and Forensics Initiative, Istanbul, Turkey*

Keywords: XAI, Explainable AI, Deep Learning, Nearest Neighbors, Neural Networks.

Abstract: Deep Learning (DL) models exhibit dramatic success in a wide variety of fields such as human-machine interaction, computer vision, speech recognition, etc. Yet, the widespread deployment of these models partly depends on earning trust in them. Understanding how DL models reach a decision can help to build trust on these systems. In this study, we present a method for explaining inaccurate predictions of DL models through post-hoc analysis of k-nearest neighbours. More specifically, we extract k-nearest neighbours from training samples for a given mispredicted test instance, and then feed them into the model as input to observe the model's response which is used for post-hoc analysis in comparison with the original mispredicted test sample. We apply our method on two different datasets, i.e. IRIS and CIFAR10, to show its feasibility on concrete examples.

1 INTRODUCTION

Explainable Artificial Intelligence (XAI) is an emerging and popular research topic in AI community, which aims to understand and explain underlying decision-making mechanism of AI-based systems (Arrieta et al., 2020). Being able to explain how AI systems reach a decision in an understandable way for human beings is crucial to build trust on these systems (Barbado and Corcho, 2019; Chakraborti et al., 2020; Ribeiro et al., 2016). This is particularly important for some use cases such as autonomous vehicles, security, finance, defense, and medical diagnosis, where an inaccurate decision could cause non-recoverable damages (Arrieta et al., 2020; Tjoa and Guan, 2019; Holzinger et al., 2019). Due to the importance of the issue, DARPA decided to launch an XAI program in May 2017, with the objective of creating AI systems whose learned models and decisions can be understood and appropriately trusted by end users (Gunning and Aha, 2019). The need for an explanation of an algorithmic decision that significantly affects human beings is also mentioned in European Union regulations (Goodman and Flaxman, 2017).

The problem actually arises from the black-box characteristics displayed by advanced AI models. Particularly, the rise of neural network-based Deep Learning (DL) models that exhibit dramatic success in a wide range of tasks from load forecasting (Ustundag Soykan et al., 2019) to vulnerability prediction (Bilgin et al., 2020), by relying on efficient learning algorithms with huge parametric space, makes them be considered as complex black-box models (Arrieta et al., 2020; Castelvecchi, 2016). Therefore, to be considered practical, a model's decision-making mechanism either needs to be more transparent, or provides hints on what could perturb the model (Hall, 2018). In this study, we focus on this issue and seek to understand why a model makes inaccurate predictions by performing experimental analysis on two different datasets from two different domains. The first dataset we consider is IRIS dataset (Dua and Graff, 2017), which consists of 50 samples from each of three species of Iris, and the second one is CIFAR10 (Krizhevsky et al., 2009), which consists of 60000 32x32 colour images in 10 different classes, with 6000 images per class. Our approach is a kind of post-hoc analysis of mispredictions based on k-nearest neighbours of training samples corresponding to inaccurately predicted test instance. Our motivation for focusing on inaccurate predictions is that explaining a model's mispredictions may be more critical with respect to accurate predictions in some situa-

[a] https://orcid.org/0000-0002-8613-4071
[b] https://orcid.org/0000-0001-8096-689X

Bilgin, Z. and Gunestas, M.
Explaining Inaccurate Predictions of Models through k-Nearest Neighbors.
DOI: 10.5220/0010257902280236
In *Proceedings of the 13th International Conference on Agents and Artificial Intelligence (ICAART 2021) - Volume 2*, pages 228-236
ISBN: 978-989-758-484-8

tions that require responsibility.

In our proposed method, when a model makes a misprediction for a certain test input, we first extract k-nearest neigbours from the training set based on a specific distance calculation approach, and then feed these extracted samples into the model as input to get auxiliary predictions which will be used for post-hoc analysis. Considering the original misprediction together with auxiliary predictions, we perform both sample-based individual analyses and collective statistical analysis on them. The main contribution of this study is that it provides a methodology, with supportive experimental results, based on the analysis of the model's behaviour on k-nearest neighbors of the mispredicted sample to understand the reasons for the model's inaccurate estimations, by presenting more appropriate distance calculation method in nearest neighbour search when dealing with image data.

The rest of the paper is organized as follows: First, in Section 2, we give an overview of related work and explain how our work differs from prior studies. Then, in Section 3, we present our post-hoc analysis method to explain inaccurate decisions of deep learning models. Section 4 includes our experimental analysis for two different datasets. Finally, we conclude our work by giving final remarks.

2 RELATED WORK

There are certain concepts that are highly related with model explainability, and some studies provide well-defined meanings of these concepts and discuss their differences. For example, in (Roscher et al., 2020), the authors review XAI in view of applications in the natural sciences and discuss three main relevant elements: *transparency*, *interpretability*, and *explainability*. *Transparency* can be considered as the opposite of the "black-boxness" (Lipton, 2018), whereas *interpretability* pertains to the capability of making sense of an obtained ML model (Roscher et al., 2020). The work (Holzinger et al., 2019) introduces the notion of *causability* as a property of a person in contrast to *explainability* which is a property of a system, and discusses their difference for medical applications. Some other studies providing comprehensive outline of the different aspects of XAI are (Chakraborti et al., 2020), (Arrieta et al., 2020) and (Cui et al., 2019).

Rule Extraction. One common and longstanding approach used to explain AI decisions is the rule extraction, which aims to construct a simpler counterpart of a complex model via approximation such as building a decision tree or linear model leading to similar predictions of the complex model. An early work in this category belongs to Ribeiro et al. (Ribeiro et al., 2016), who present a method to explain the predictions of any model by learning an interpretable sparse linear model in a local region around the prediction. In another work (Barbado and Corcho, 2019), the authors evaluate some of the most important rule extraction techniques over the OneClass SVM model which is a method for unsupervised anomaly detection. In addition, they propose algorithms to compute metrics related with XAI regarding the "comprehensivility", "representativeness", "stability" and "diversity" of the rules extracted. The works (Bologna and Hayashi, 2017; Bologna, 2019; Bologna and Fossati, 2020) present a few different variants of a similar propositional rule extraction technique from several neural network models trained for various tasks such as sentiment analysis, image classification, etc.

Post-hoc Analysis. Another widely adopted approach is the post-hoc analysis, which involves different techniques trying to explain the predictions of ML models that are not transparent by design. In this category, the authors of (Petkovic et al., 2018) develop frameworks for post-training analysis of a trained random forest with the objective of explaining the model's behavior. Adopting a user-centered approach, they generate an easy to interpret one page *explainability summary report* from the trained RF classifier, and claim that the reports dramatically boosted the user's understanding of the model and trust in the system. In another study (Hendricks et al., 2016), the authors bring a visual explanation method that focuses on the discriminating properties of the visible object, jointly predicts a class label, and explains why the predicted label is appropriate for the image.

A model explanation technique relevant to our proposed method is the *explanation by example* as a subcategory of the post-hoc analysis approach (Arrieta et al., 2020). As an early work in this category, Bien et al. (Bien and Tibshirani, 2011) develop a Prototype Selection (PS) method, where a prototype can be considered as a very close or identical observation in the training set, that seeks a minimal representative subset of samples with the objective of making the dataset more easily "human-readable". Aligned with (Bien and Tibshirani, 2011), Li et al. (Li et al., 2018) use prototypes to design an interpretable neural network architecture whose predictions are based on the similarity of the input to a small set of prototypes. Similarly, Caruena et al. (Caruana et al., 1999) suggest that a comparison of the representation predicted by a single layer neural network with the representations learned on its training data would help identify points in the training data that best explain the prediction made. The work (Papernot and McDaniel, 2018) exhibits a particular example of classical ML model enhanced with its DL counterpart (Deep Nearest Neighbors DkNN), where the neighbors constitute human-interpretable explanations of predictions including model failures. Our own study differs from these studies in that (i) we focus on diagnosing possible root causes of a model's inaccurate predictions and thus try to explain what perturbs the model, (ii) we do not design a new neural network structure (e.g. on contrary to (Li et al., 2018)), (iii) we perform post-hoc analyses based on the model's extra predictions when the k-nearest neighbors of training samples of the mispredicted test inputs are entered into the model, and (iv) we find k-nearest neighbors based on the distance calculated according to the features extracted at internal layer of convolutional neural network (CNN) used.

3 EXPLAINING INACCURATE PREDICTIONS VIA k-NEAREST NEIGHBORS

Our objective is to understand why a model makes inaccurate prediction on a certain test sample. If this goal is achieved, the model can be improved by taking appropriate actions based on revealed root causes of the inaccurate predictions. To this end, we present a post-hoc analysis method based on analysis of the model's prediction response on k-nearest neighbors of the training samples corresponding to the test sample in question. To put it another way, we first extract the k-nearest neighbors from the training dataset for a given mispredicted test input, and then feed these extracted k-nearest neighbors into the same model and get the auxiliary predictions for these extracted k-nearest neighbors. Then, we perform post-hoc analyses on these additional predictions together with original inaccurate test prediction by seeking to reveal what could perturb the model. Figure 1 depicts high-level schema of our methodology.

As depicted in Figure 1, our method relies on extracting k-nearest neighbors from training dataset for a given test input, and therefore, it is highly crucial for our method how to calculate distance between two samples, which forms the basis of the nearness criterion between the two samples. In the following subsection, we discuss this issue in detail from the perspective of two different datasets in two different domains.

Table 1: Sample instances from IRIS dataset.

Flower Name	Attributes: sepal length (cm)	sepal width (cm)	petal length (cm)	petal width (cm)
Setosa	5.1	3.5	1.4	0.2
Setosa	4.9	3.0	1.4	0.2
Versicolor	7.0	3.2	4.7	1.4
Versicolor	5.5	2.3	4.0	1.3
Virginica	6.3	3.3	6.0	2.5
Virginica	5.8	2.7	5.1	1.9

Table 2: 3-nearest neighbours of a sample based on euclidean distance in IRIS dataset.

Flower Name	Attributes: sepal length (cm)	sepal width (cm)	petal length (cm)	petal width (cm)	Nearest Neighbors: euclidean distance (cm)
Setosa	5.1	3.5	1.4	0.2	-
Setosa	5.1	3.5	1.4	0.3	0.100
Setosa	5.0	3.6	1.4	0.2	0.141
Setosa	5.1	3.4	1.5	0.2	0.141

3.1 Extracting k-Nearest Neighbors

There are many alternative metrics that can be used to measure distance between two samples. For example, one of the most widely used metric is euclidean distance, which calculates element-wise distance between corresponding elements of two item to be compared as formulated in Equation 1.

$$L(x,y) = \sqrt{\sum_{i=1}^{n}(x_i - y_i)^2} \quad (1)$$

where x and y are a pair of samples in an n-dimensional feature space.

Euclidean distance can be safely used to measure distance between two samples especially when these samples are constituted of features with numeric values. For example, in IRIS dataset, each instance is represented with four features as indicated in Table 1. These are sepal length, sepal width, petal length, and petal width in cm of the iris flower. The euclidean-based 3-nearest neighbours of the first instance in Table 1 are given in Table 2. For this particular case, it is easy to observe the similarity between the given instance and its nearest neighbours as there are small deviations on some of the feature values.

However, when we deal with an image dataset such as CIFAR10, calculating euclidean distance directly between two images may not be appropriate to

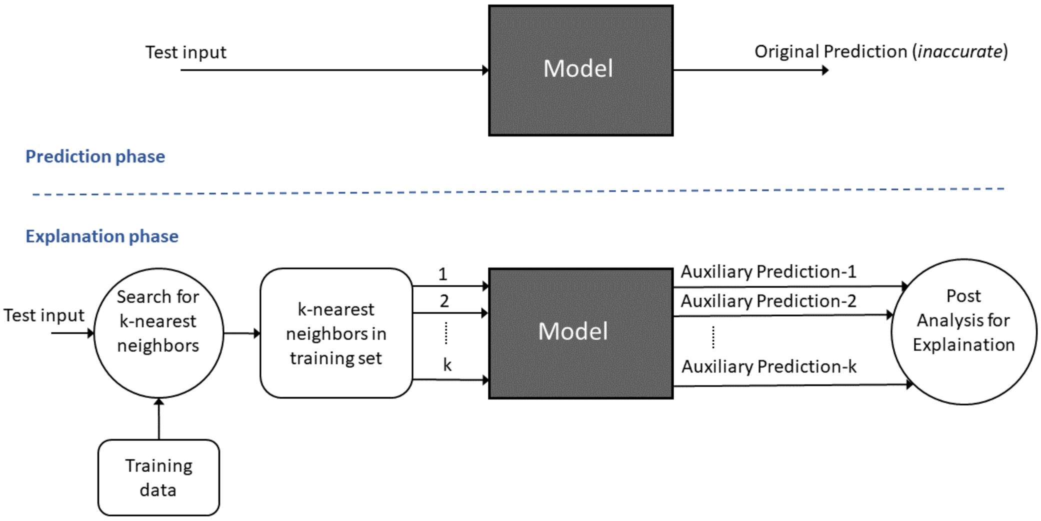

Figure 1: Overview of the method.

find nearest neighbours. This is because the similarity between two images is something complicated and requires sophisticated analysis. For example, consider two images consisting of the same object but in different locality in the images (e.g. the object is located in top-left of the first image, whereas it is in the bottom-right of the second image). In such a case, the euclidean distance between these two images could be a large number, implying that these two images have not any common property, although the opposite is the case. To illustrate this, as an example, we found 3-nearest neighbours of an image from CIFAR10 dataset based on euclidean distance between images, and demonstrate them in Figure 2a.

As seen in Figure 2a, the 3-nearest neighbours of the given test sample (index=0 in the original CIFAR10 test dataset) are images of deer, bird, and bird respectively, which validates our claim that similarity between images is a bit more complicated than similarity between vectoral data. Therefore, while finding nearest neighbours in CIFAR10 dataset, instead of directly applying euclidean distance calculation on images, we first get the extracted image features at internal layers of the utilized convolutional neural network as depicted in Figure 3, and then calculate euclidean distance on these features which is in the form of a vector consisting of numeric data. We hypothesise that this approach could give more meaningful and appropriate nearest neighbours. To validate this, for the same test sample given in Figure 2a, we found the 3-nearest neighbours based on the euclidean distance between the extracted features at the internal layers of the neural network as demonstrated in Figure 2b. As seen in Figure 2b, the 1^{st} and 3^{rd} nearest neighbours are images of a cat, which really look like the test sample, and the 2^{nd} nearest neighbour is an image of deer, which is also meaningful as it has observable similar patterns (e.g. curves) with the test sample. As a result, when dealing with CIFAR10 dataset, we find nearest neighbours based on euclidean distance between the extracted features at internal layers of the neural network to be used.

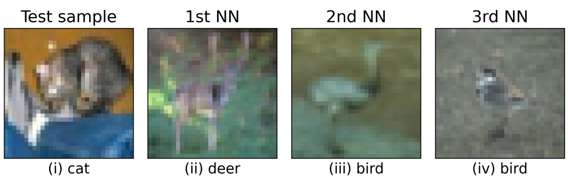

(a)

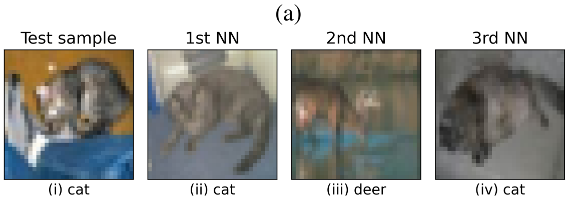

(b)

Figure 2: The 3-nearest neighbours of the training set for the very first sample of the test set in CIFAR10 dataset based on (a) euclidean distance directly between images and (b) euclidean distance on the extracted features at the internal layers of the neural network.

3.2 Post-hoc Analysis

When we encounter an incorrect prediction of the model, we first extract the k-nearest neighbours in the training set based on the incorrectly predicted test sample as described in the previous part, and then give them as input to the model in order to obtain auxiliary

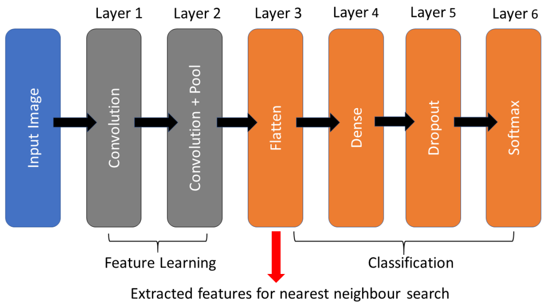

Figure 3: Getting the features extracted at the internal layers of CNN, which is used for distance calculations in k-nearest neighbor search.

predictions. In the post-hoc analyses, we compare the original inaccurate prediction with the auxiliary predictions with the objective of revealing possible cause of the misprediction in question. There may appear different cases as explained below:

- **Case-I:** A sample of k-nearest neighbour is belong to same category with the corresponding inaccurately predicted test sample, and the model makes accurate prediction when this nearest neighbour is given the model as input. This situation is a sign that the model actually fits well and inaccurate prediction of the test sample is an unexpected circumstance.
- **Case-II:** A sample of k-nearest neighbour is belong to same category with the corresponding inaccurately predicted test sample, but the model makes inaccurate prediction when this nearest neighbour is given the model as input. This situation implies that the model may not be fitted very well which could also be the root cause of the original misprediction of the test sample.
- **Case-III:** A sample of k-nearest neighbour is belong to different category with respect to the corresponding inaccurately predicted test sample, and the model makes accurate prediction when this nearest neighbour is given the model as input. This situation can imply that this nearest neighbour may have some disruptive effect on the model's prediction performance on the test sample in question, because the fact that the model makes accurate prediction on a nearest neighbour in different category means that the model learnt to yield this nearest neighbour's category when identical inputs are given, which would be an inaccurate prediction for the corresponding test input. On the other hand, if the majority of the nearest neighbours falls in this case, then the mispredicted test instance is likely to be an outlier or located near the boundaries of data points.
- **Case-IV:** A sample of k-nearest neighbour is belong to different category with respect to the corresponding inaccurately predicted test sample, and the model makes inaccurate prediction when this nearest neighbour is given the model as input. How this situation affects the model's behaviour on the related test sample partly depends on whether this misprediction of the nearest neighbour is the same with the original inaccurate test prediction or not. For Case IV, suppose the model's prediction for the nearest neighbour is different than the original test misprediction. This situation does not give any clue about the model's inaccurate prediction for the test sample.
- **Case-V:** A sample of k-nearest neighbour is belong to different category with respect to the corresponding inaccurately predicted test sample, and the model makes inaccurate prediction when this nearest neighbour is given the model as input. Moreover, this misprediction is the same with the original test misprediction. Such a situation implies that the model behaves in harmony with the nearest neighbours, and may also point that the test sample is outlier of its own category.

4 EXPERIMENTAL ANALYSIS

We realized our implementation in the scikit-learn machine learning platform (Pedregosa et al., 2011), and applied our explanation method on two different datasets as described in detail in the following subsections.

4.1 IRIS Dataset

IRIS dataset (Fisher, 1936) contains 3 classes of 50 instances each, where each class refers to a type of iris plant, with four attributes as shown in Table 1. This is a pretty simple dataset for classification task and can be successfully handled by using simple machine learning algorithms, without requiring any neural network implementation. However, we intentionally preferred to use this dataset in our neural network based experimental analysis because we believe it can serve our purpose well thanks to its simplicity.

In our neural network implementation, we included 1 hidden layer with 12 neurons, and splitted whole dataset into training and test sets with 2/3 and 1/3 ratio respectively. We trained the model up to the optimal epoch where minimum validation loss is achieved, which allows us to avoid underfitting or overfitting situations.

4.1.1 Sample-based Analysis

After completing the model training, we performed predictions on test dataset, and picked an inaccurate prediction for post-hoc analysis. Table 3 shows mispredicted test instance along with associated 11-nearest neighbor instances from training dataset. As seen in Table 3, the majority of the 11-nearest neighbours fall into Case III, which implies that the mispredicted test sample is likely to be an outlier or located near the boundaries of data points as justified in Section 3.2. To examine this issue a little more, we plotted 2D views of IRIS dataset as seen in Figure 4. Figure 4a shows 2D view of IRIS data from the perspective of the attribute pair of "sepal width" and "sepal length", where the mispredicted sample, which is normally belong to the category of "versicolor", is colored red. It is seen from Figure 4a that the mispredicted sample is located among "versicolor" and "virginica" samples that makes it difficult to distinguish. On the other hand, Figure 4b shows 2D view of IRIS data from the perspective of the attribute pair of "petal width" and "petal length", where the mispredicted sample is again colored red. It is seen from Figure 4b that the mispredicted sample is located near the boundary between "versicolor" and "virginica" samples, which makes it clear why the model made inaccurate prediction on this specific sample. This is compatible with our posthoc analysis and interpretations that we have done above.

4.1.2 Statistical Analysis

In our experiments, 2 test samples out of 50 were mispredicted by the model, one of which have been explained in the previous part. In this part, we provide statistical distribution of k-nearest neighbors based posthoc analysis of these two mispredicted test samples. Figure 5 shows distribution as percentage of the 11-nearest neighbors of the two mispredicted test samples according to the cases in our posthoc analysis. As seen in Figure 5, the majority of the 11-nearest neighbors fall into Case-III, which implies that the mispredicted test samples are either outliers or located near boudaries.

4.2 CIFAR10 Dataset

The CIFAR-10 dataset consists of 60000 32x32 colour images in 10 different classes, with 6000 images per class, which are splitted as 50000:10000 for training and test purposes. The 10 classes in CIFAR-10 represent airplanes, cars, birds, cats, deer, dogs, frogs, horses, ships, and trucks.

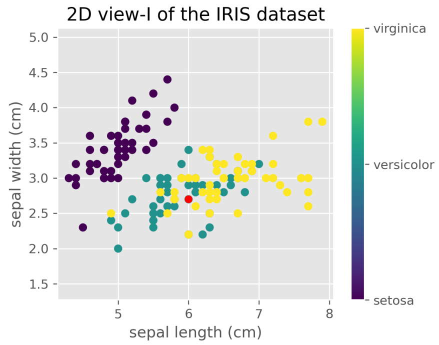

(a)

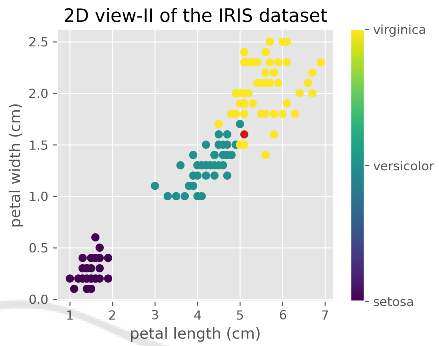

(b)

Figure 4: 2D views of IRIS dataset based on pairs of attributes. The red circle represents the mispredicted sample which is normally belong to category of "versicolor".

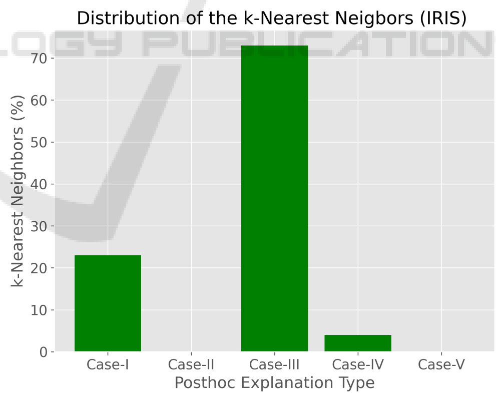

Figure 5: Distribution of the 11-nearest neighbours of the training set corresponding to inaccurate test samples when they are given as input to the model.

In our experimental analysis, we implemented a CNN which has similar architecture with VGG as follows: Two successive 2D convolutional layers with 32 filters and kernel size of (3,3), followed by pooling layer and flatten layer. Then a dense layer with 128 neurons followed by a droput layer and finally final dense layer with softmax function. We trained the model up to the optimal epoch where minimum validation loss

Table 3: 11-nearest neighbours of a sample based on euclidean distance in IRIS dataset.

Instance	Attributes				Distance	Prediction	True Label	Explanation
Type	sepal length (cm)	sepal width (cm)	petal length (cm)	petal width (cm)	euclidean (cm)			
Test	6.0	2.7	5.1	1.6	-	virginica	versicolor	
1^{st} NN	6.3	2.8	5.1	1.5	0.450	versicolor	virginica	Case IV
2^{nd} NN	6.3	2.7	4.9	1.8	0.462	virginica	virginica	Case III
3^{rd} NN	5.8	2.7	5.1	1.9	0.463	virginica	virginica	Case III
4^{rt} NN	5.8	2.7	5.1	1.9	0.463	virginica	virginica	Case III
5^{th} NN	6.3	2.5	4.9	1.5	0.612	versicolor	versicolor	Case I
6^{th} NN	6.4	2.7	5.3	1.9	0.635	virginica	virginica	Case III
7^{th} NN	5.7	2.8	4.5	1.3	0.676	versicolor	versicolor	Case I
8^{th} NN	6.3	2.9	5.6	1.8	0.703	virginica	virginica	Case III
9^{th} NN	6.3	2.5	5.0	1.9	0.709	virginica	virginica	Case III
10^{th} NN	5.9	3.0	5.1	1.8	0.749	virginica	virginica	Case III
11^{th} NN	6.0	3.0	4.8	1.8	0.758	virginica	virginica	Case III

is achieved, which allows us to avoid underfitting or overfitting situations.

4.2.1 Sample-based Analysis

After completing the model training, we performed predictions on test dataset, and picked an inaccurate prediction for post-hoc analysis. Figure 6 shows the mispredicted test sample along with its 11-nearest neighbours from training dataset. The caption under each subfigure indicates true label of the given figure and the model's prediction when this image is given as input.

As seen in Figure 6, the original test image contains a frog, but the model inaccurately classified this sample as an deer image. When we look at the 11-nearest neighbours, 1st, 2nd, 3rd, 4rt, 7th, 8th, 9th, 10th and 11th nearest neigbours (9 out of 11) fall into Case III according to explanations given in Section 3.2, which implies that the model behaved in harmony with the nearest neighbors for this specific test sample.

4.2.2 Statistical Analysis

In our experiments, the validation accuracy of the model was about 68.61%, which corresponds to 3139 inaccurate predictions given that there are 10000 test instances in CIFAR10 datasets. Taking k=3 in k-nearest neighbors, we find k-nearest neighbors for all mispredicted test instances, and then performed posthoc analysis according to explanations given in Section 3.2. Figure 7 shows statistical distribution of k-nearest neighbors according to the cases given in our posthoc analysis.

As seen in Figure 7, almost 50% of the k-nearest neighbors fall into Case-III, which implies that the mispredicted test instances are likely to be outliers or located near the boundaries of data points.

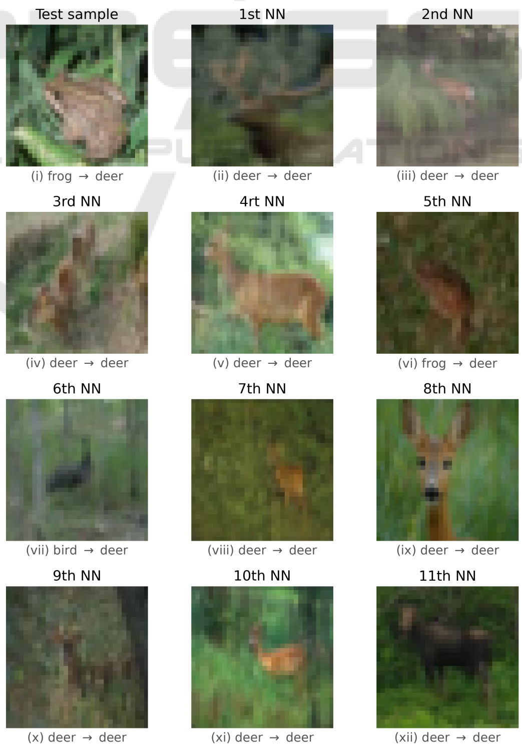

Figure 6: The 11-nearest neighbours in the training set for a mispredicted test sample based on euclidean distance on the extracted features at the internal layers of the neural network.

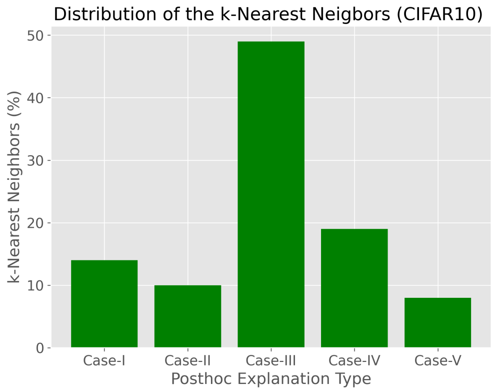

Figure 7: Distribution of the 3-nearest neighbours of the training set corresponding to inaccurate test samples when they are given as input to the model.

5 CONCLUSION

We studied the root causes of inaccurate decisions reached particularly by deep learning models, which is an important issue for many use cases that require responsibility for the actions taken by AI. We developed a method for finding k-nearest neighbours in training set for a given test instance, which were enhanced for finding similar images such that we calculate euclidean distance not directly on the compared images, but instead, on the features extracted from internal layers of the convolutional neural network. To reveal possible root cause of an inaccurate prediction, we thus find k-nearest neighbours from training samples and re-entered them into the model to observe its behaviour for further analysis. By comparing the model's responses on the k-nearest neighbours and the associated test input, we estimated possible root cause of the mispredictions. We validated our proposed method on both IRIS and CIFAR-10 datasets, and experimentally showed that our proposed method can be used to understand why a model makes inaccurate misprediction.

REFERENCES

Arrieta, A. B., Díaz-Rodríguez, N., Del Ser, J., Bennetot, A., Tabik, S., Barbado, A., García, S., Gil-López, S., Molina, D., Benjamins, R., et al. (2020). Explainable artificial intelligence (xai): Concepts, taxonomies, opportunities and challenges toward responsible ai. *Information Fusion*, 58:82–115.

Barbado, A. and Corcho, Ó. (2019). Rule extraction in unsupervised anomaly detection for model explainability: Application to oneclass svm. *arXiv preprint arXiv:1911.09315*.

Bien, J. and Tibshirani, R. (2011). Prototype selection for interpretable classification. *The Annals of Applied Statistics*, pages 2403–2424.

Bilgin, Z., Ersoy, M. A., Soykan, E. U., Tomur, E., Çomak, P., and Karaçay, L. (2020). Vulnerability prediction from source code using machine learning. *IEEE Access*, 8:150672–150684.

Bologna, G. (2019). A simple convolutional neural network with rule extraction. *Applied Sciences*, 9(12):2411.

Bologna, G. and Fossati, S. (2020). A two-step rule-extraction technique for a cnn. *Electronics*, 9(6):990.

Bologna, G. and Hayashi, Y. (2017). Characterization of symbolic rules embedded in deep dimlp networks: a challenge to transparency of deep learning. *Journal of Artificial Intelligence and Soft Computing Research*, 7(4):265–286.

Caruana, R., Kangarloo, H., Dionisio, J., Sinha, U., and Johnson, D. (1999). Case-based explanation of non-case-based learning methods. In *Proceedings of the AMIA Symposium*, page 212. American Medical Informatics Association.

Castelvecchi, D. (2016). Can we open the black box of ai? *Nature News*, 538(7623):20.

Chakraborti, T., Sreedharan, S., and Kambhampati, S. (2020). The emerging landscape of explainable ai planning and decision making. *arXiv preprint arXiv:2002.11697*.

Cui, X., Lee, J. M., and Hsieh, J. (2019). An integrative 3c evaluation framework for explainable artificial intelligence.

Dua, D. and Graff, C. (2017). UCI machine learning repository.

Fisher, R. A. (1936). The use of multiple measurements in taxonomic problems. *Annals of eugenics*, 7(2):179–188.

Goodman, B. and Flaxman, S. (2017). European union regulations on algorithmic decision-making and a "right to explanation". *AI magazine*, 38(3):50–57.

Gunning, D. and Aha, D. W. (2019). Darpa's explainable artificial intelligence program. *AI Magazine*, 40(2):44–58.

Hall, P. (2018). On the art and science of machine learning explanations. *arXiv preprint arXiv:1810.02909*.

Hendricks, L. A., Akata, Z., Rohrbach, M., Donahue, J., Schiele, B., and Darrell, T. (2016). Generating visual explanations. In *European Conference on Computer Vision*, pages 3–19. Springer.

Holzinger, A., Langs, G., Denk, H., Zatloukal, K., and Müller, H. (2019). Causability and explainability of artificial intelligence in medicine. *Wiley Interdisciplinary Reviews: Data Mining and Knowledge Discovery*, 9(4):e1312.

Krizhevsky, A., Hinton, G., et al. (2009). Learning multiple layers of features from tiny images.

Li, O., Liu, H., Chen, C., and Rudin, C. (2018). Deep learning for case-based reasoning through prototypes: A neural network that explains its predictions. In *Thirty-second AAAI conference on artificial intelligence*.

Lipton, Z. C. (2018). The mythos of model interpretability. *Queue*, 16(3):31–57.

Papernot, N. and McDaniel, P. (2018). Deep k-nearest neighbors: Towards confident, interpretable and robust deep learning. *arXiv preprint arXiv:1803.04765*.

Pedregosa, F., Varoquaux, G., Gramfort, A., Michel, V., Thirion, B., Grisel, O., Blondel, M., Prettenhofer, P., Weiss, R., Dubourg, V., Vanderplas, J., Passos, A., Cournapeau, D., Brucher, M., Perrot, M., and Duchesnay, E. (2011). Scikit-learn: Machine learning in Python. *Journal of Machine Learning Research*, 12:2825–2830.

Petkovic, D., Altman, R. B., Wong, M., and Vigil, A. (2018). Improving the explainability of random forest classifier-user centered approach. In *PSB*, pages 204–215. World Scientific.

Ribeiro, M. T., Singh, S., and Guestrin, C. (2016). " why should i trust you?" explaining the predictions of any classifier. In *Proceedings of the 22nd ACM SIGKDD international conference on knowledge discovery and data mining*, pages 1135–1144.

Roscher, R., Bohn, B., Duarte, M. F., and Garcke, J. (2020). Explainable machine learning for scientific insights and discoveries. *IEEE Access*, 8:42200–42216.

Tjoa, E. and Guan, C. (2019). A survey on explainable artificial intelligence (xai): towards medical xai. *arXiv preprint arXiv:1907.07374*.

Ustundag Soykan, E., Bilgin, Z., Ersoy, M. A., and Tomur, E. (2019). Differentially private deep learning for load forecasting on smart grid. In *2019 IEEE Globecom Workshops (GC Wkshps)*, pages 1–6.